Bayesian-optimized deep learning for predicting compressive strength of sustainable eggshell foamed concrete

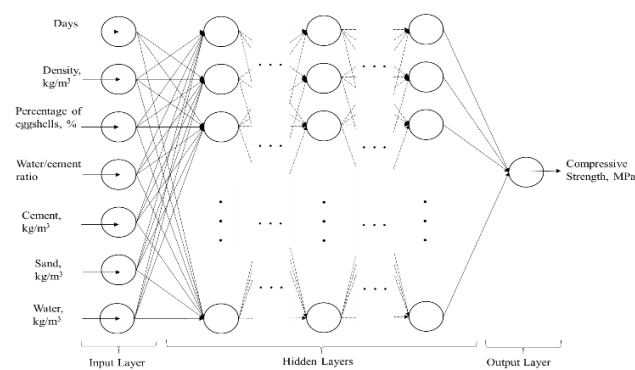**Lim M.H.[1]*, Siong Kang Lim [1], Yee Ling Lee.[1], Kim Yee Lee.[1] and Hock Yong Tiong.[1]**
[1]Department of Civil Engineering, Lee Kong Chian Faculty of Engineering & Science, Universiti Tunku Abdul Rahman (UTAR) Sungai Long Campus, Jalan Sungai Long, 43000 Kajang, Malaysia
*to whom all correspondence should be addressed: e-mail: limmh@utar.edu.my

Graphical abstract

Abstract

The use of eggshell-based foamed concrete represents a sustainable approach to enhancing environmental friendliness in construction materials. This study investigates the predictive modelling of the compressive strength of eggshell-based foamed concrete through a deep learning model, fine-tuned via Bayesian optimization. Utilizing a dataset of 360 samples with diverse input parameters, the model was optimized with four hidden layers (28, 21, 28, and 21 neurons) and the Rectified Linear Unit (ReLU) activation function. The model demonstrated excellent predictive accuracy, achieving a mean squared error of 0.0522, a mean absolute error of 0.0382, and an R^2 value of 0.9548 over 200 epochs. Notably, the water/cement ratio emerged as the most influential factor in prediction accuracy. This research provides a robust, AI-driven method for predicting the compressive strength of sustainable construction materials, contributing to advancements in environmental technology and the optimization of eco-friendly construction practices.

Keywords: Waste eggshell powder, compressive strength, deep learning, hyperparameter tuning

1. Introduction

Lightweight foamed concrete (LFC) has a variety of uses as low-density concrete in the construction industry (Mydin et al. 2022; Suhaili et al. 2021; Pirah et al. 2022). LFC performs well in compression but poorly in bending and tensile stresses because it develops multiple microcracks and cannot sustain the further stress brought on by applied forces without additional reinforcing elements. To improve the mechanical properties of LFC, researchers have looked into the use of a variety of materials, including oil palm spikelets, empty fruit bunch fibre, fibreglass mesh netting, and alkali-resistant woven fibre mesh (Mydin et al. 2022; Suhaili et al. 2021; Pirah et al. 2022; Mydin, 2023; Serudin et al. 2022). There are many benefits to using LFC in construction. According to Villiers and Petrus (2016), LFC is a low-density concrete that uses the entrapment of air produced by a protein-based foam mix constituent to make it lighter than conventional concrete. LFC can be made by foaming the mortar to produce porous and lightweight concrete (Sumiati et al. 2020). According to Sumiati et al. (2020), the lightweight nature of LFC provides some advantages, including reducing bending moments and helping to mitigate earthquakes. However, cement is used in the creation of foamed concrete as a binding agent, which has a significant amount of carbon footprint (Othman et al. 2023). Therefore, there has been a rise in interest in researching cement alternatives to enhance resource efficiency, energy efficiency, and overall foamed concrete properties (Othman et al. 2023).

To explore the possibilities for cement alternatives, the waste materials can be used as a substitute for cement in foamed concrete. Soil, for instance, can be utilised as a filler in foamed concrete, a novel lightweight construction material made of cement, soil, water, and a foaming agent (Kavya et al. 2020). Red mud magnesium oxysulfate cement, mussel shell, palm oil fuel ash, and used cooking oil foaming agents were a few other waste materials that have been investigated for usage in LFC (Rahman et al. 2021; Shah et al. 2021; Hafiz et al. 2014). Likewise, the LFC can be considered a sustainable construction material that uses waste by-products as lightweight coarse aggregates, including oil palm shells and crushed clay bricks (Sumiati et al. 2020; Liu et al. 2014). The mechanical properties of LFC can be improved by the inclusion of reinforcing

materials, such as fibreglass mesh netting and empty fruit bunch fibre from oil palms (Mydin *et al.* 2022; Mydin, 2023). Overall, the usage of LFC may contribute to natural resource conservation, the reduction of environmental issues, and increased concrete construction durability.

Eggshell waste is a common by-product of daily living that can be recycled to help with waste disposal issues and to encourage the use of LFC (Tiong *et al.* 2018). Eggshell powder is used as a partial replacement for standard Portland cement in Eggshell-based Foamed Concrete (EFC), a type of lightweight concrete. EFC is recognized as an environmentally friendly and sustainable building material due to its use of eggshell waste and other agro-industrial wastes, such as palm oil fuel ash, as supplementary cementitious ingredients. According to studies, the ideal range for eggshell powder inclusion in EFC is between 5% and 15% (Tiong *et al.* 2022; Jhatial *et al.* 2021b; Lim *et al.* 2021; Jhatial *et al.* 2020; Rahman *et al.* 2019). The optimum mixture of EFC varies depending on the desired properties and application. According to previous studies, adding 5% eggshell powder as a partial cement replacement material enhances the initial surface absorption, sorptivity, and dimensional stability of LFC (Tiong *et al.* 2022; Lim *et al.* 2021). In another study, it was discovered that adding supplementary cementitious materials to foamed concrete, such as 5% – 15% eggshell powder and 30% – 35% palm oil fuel ash, produced favourable results in terms of thermal insulation and mechanical strength (Jhatial *et al.* 2021b; Jhatial *et al.* 2020). In addition, a study discovered that the LFC mixture with 5% eggshell powder produced optimal results for assessing its acoustic qualities at a water-to-cement ratio of 0.6 (Tiong *et al.* 2022). The optimal EFC mixture will therefore rely on the specific application and desired properties. Additionally, using eggshell powder as a supplementary cementitious material in foamed concrete may aid sustainability efforts by minimising waste and carbon impact (Rahman *et al.* 2019; Jhatial *et al.* 2021a). The pozzolanic property of eggshell powder can help to generate C-S-H gels, which can boost the strength of foamed concrete. Eggshell powder is also a less expensive alternative to ordinary Portland cement (Jhatial *et al.* 2021a).

Numerous studies have been conducted to develop prediction models for the compressive strength of foamed concrete. Some of these models take into account variables like the composition of the mix, the duration of the curing process, and porosity (Zhao *et al.* 2018), whereas other models employ artificial neural networks to forecast compressive strength based on input variables like density, water-cement ratio, and sand-cement ratio (Singh *et al.* 2021). Another study uses an adaptive neuro-fuzzy inference system, optimized with nature-inspired algorithms, to predict compressive strength (Sharafati *et al.* 2021). These studies aim to improve the accuracy and precision of predicting the compressive strength of foamed concrete, which can help optimize the mix composition and casting density of the concrete. Several factors affect the performance of foamed concrete

strength prediction. According to Falliano *et al.* (2018), foamed concrete can achieve some degree of strength depending on the density, foaming agent, and water-cement ratio. Ghahremani *et al.* (2023) examined the impact of pore size and shape on the prediction model for the compressive strength of foamed concrete. According to Retamal and Rougier (2021), density has a major influence on the compressive strength of foamed concrete, followed by the water-to-cement and sand-to-cement ratios. The compressive strength of high-porosity cast-in-situ foamed concrete was also found to be influenced by the curing time, mix composition, and porosity (Zhao *et al.* 2018; Wong *et al.* 2019). Therefore, to accurately predict the compressive strength of foamed concrete, it is necessary to consider factors such as density, water-cement ratio, foaming agent, curing time, mix constitution, and porosity.

Recent research has looked into the application of deep learning methods to concrete compressive strength prediction. Ali *et al.* (2024) conducted comprehensive studies on AI-based prediction methods for self-compacting, geopolymer, and other eco-friendly concrete types. Falah *et al.* (2022) utilized a deep learning neural network to model the compressive strength of eco-friendly concrete incorporating recycled aggregates. De-Prado-Gil *et al.* (2022) applied deep learning techniques to predict the splitting tensile strength of self-compacting recycled aggregate concrete. Mahmood *et al.* (2023) used both machine learning and deep learning techniques to enhance the compressive strength prediction of self-compacting concrete containing rice husk ash and marble powder. Similarly, Gao and Ma (2024) predicted and simulated the compressive strength of concrete in which cement and fine aggregate were replaced with waste materials such as eggshell powder (ESP) and waste glass powder (WGP) for sustainable construction. In addition, Khan *et al.* (2023) developed machine learning-based models to predict the water absorption capacity of cement mortar with eggshell powder as a cement replacement. The effectiveness of deep learning in predicting concrete strength has been shown in these studies. However, to date, no study has explored the use of deep learning for predicting the compressive strength of EFC. Accordingly, this paper presents a deep learning model optimized through Bayesian optimization for predicting the compressive strength of EFC. Various mix proportions of EFC were prepared as training, validation and testing data for the deep learning model to predict the compressive strength. The hyperparameters of the model were tuned to achieve optimal performance, which can be utilized as a prediction tool for researchers in designing EFC in future studies.

2. Material and methods

2.1. Preparation of materials

The materials used for the EFC included ordinary Portland cement (OPC), fine sand, eggshell powder, foam, and water. The OPC used was a locally branded Type I Portland Cement in accordance with ASTM C 150 (2012)

and MS EN 197-1 (2014), with a strength of 52.5 N. The designation 52.5 N refers to the strength class, indicating that the OPC paste is expected to achieve a compressive strength of 52.5 MPa at 28 days. The cement was sieved at a size of 300 micrometers to ensure consistency and uniformity in the mixture. The eggshell powder was prepared by cleaning and drying the eggshells under the hot sun, followed by crushing, grinding, and sieving to a size of less than 63 μm. The fine sand used complied with ASTM C 778 (2021), BS EN 12620 (2013) and ASTM C33 (2023), and was dried in an oven at 105 °C for 24 hours before being sieved to a size not more than 600 μm (Lim *et al.* 2015). Tap water was used as the mixing water, and a synthetic foaming agent, poly-oxyethylene alkyether sulfate, was used to create the stable foam at the density of 45 kg/m3 required for the foamed concrete. These materials were carefully selected and prepared to ensure consistency and accuracy in the mixture, resulting in a high-quality EFC suitable for deep learning prediction model training, validation and testing. **Figure 1** illustrates the material preparation, casting, and compressive strength testing process. First, the dry materials, including OPC, sieved sand, and ground eggshell powder, were thoroughly mixed until uniform. Water was then gradually added to the dry mix and stirred continuously until fully incorporated, forming a slurry cement paste. Meanwhile, the foaming agent and water were introduced into the foam generator, with the pressure set to 0.5 MPa. Once the pressure stabilized at 0.5 MPa, foam was extracted and transferred to a bucket. The foam was then gently mixed into the slurry to avoid damage. After achieving a uniform mix, the concrete was poured into a 1-litre container to check the fresh density and ensure it met the target density. The slurry foamed concrete was then poured into oiled moulds and left to set for 24 hours. After setting, the hardened foamed concrete was demoulded and cured in a water tank for 7 and 28 days. Upon completion of curing, the foamed concrete was

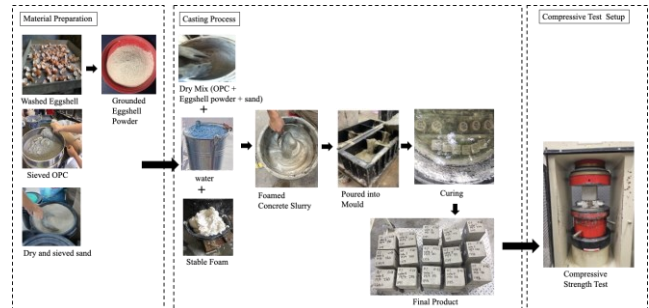tested for compressive strength according to BS EN 12390-3 (2002), using a constant loading rate of 0.1 kN/s.

Figure 1. Process of Material, Casting and Compressive Strength Test

2.2. Mix design for eggshell-based foamed concrete

A total of 360 EFC cubes (100 mm x 100 mm x 100 mm) were prepared for training and validating the deep learning model. The mix design of the specimens was varied based on the density of the concrete, the replacement percentage of eggshell to replace cement, and the water-to-cement ratio. Four different densities, namely 800 kg/m³, 1000 kg/m³, 1200 kg/m³, and 1400 kg/m³, were tested. For each density, five different percentages of eggshell replacements were tested, ranging from 0%

to 10% at an increment of 2.5%. Furthermore, for each eggshell replacement percentage, three different water-to-cement ratios were tested, which were 0.56, 0.60, and 0.64. For each water-to-cement ratio, three samples were tested at both 7 days and 28 days, resulting in a total of 360 samples. The mix design was carefully planned to ensure that a comprehensive dataset was generated for training, validation and testing the deep learning model. The results obtained from the mix design experimentation on the EFC cubes are presented in Table 1, which highlights a selection of five datasets randomly chosen from the total pool of 360 datasets.

Table 1. Randomly Selected Datasets from the Mix Design

Day	Density, kg/m³	Percentage of eggshells, %	Water/Cement Ratio	Cement, kg/m³*	Sand, kg/m³*	Water, kg/m³*	Compressive Strength, MPa
28	800	0.0	0.64	303	303	194	1.14
7	1000	7.5	0.56	391	391	219	1.26
28	1000	7.5	0.64	379	379	242	1.83
7	1200	10.0	0.56	469	469	263	2.62
28	1400	10.0	0.60	538	538	323	5.98

The weight of material used in producing 1 m³ foamed concrete.

2.3. Statistical and descriptive analysis on the datasets

This section presents the statistical and descriptive analysis of the EFC datasets. Table 2 summarizes the statistical analysis of key parameters measured in the eggshell foamed concrete samples, providing an overview of the maximum, minimum, mean, median, mode, standard deviation, and variance values. These parameters include curing days, density, eggshell replacement percentage, water/cement ratio, cement, sand, water, and compressive strength. The curing period

ranged from 7 days to 28 days, with a mean of 17.5 days. Density values varied from 800 kg/m³ to 1400 kg/m³, with an average of 1100 kg/m³. Eggshell replacement was tested from 0% to 10%, averaging at 5%, while the water/cement ratio ranged from 0.56 to 0.64, placing around a mean of 0.60. Cement content ranged from 331 kg/m³ to 547 kg/m³, sand from 294 kg/m³ to 547 kg/m³, and water content from 194 kg/m³ to 339 kg/m³. The compressive strength values show considerable variation, with a maximum strength of 8.69 MPa and a minimum of

0.53 MPa, averaging at 3.05 MPa. Standard deviation and variance values indicate the distribution and variability within each parameter, highlighting the spread across the dataset. For better visualization, **Figures 2 and 3(a)** show the statistical analysis of input and output parameters,

whilst **Figure 3(b)** illustrates the frequency distribution of compressive strengths. It provides an essential baseline for understanding the material properties of the eggshell foamed concrete samples across various mix designs.

Table 2. Statistical Characteristics of the Datasets

Parameters	Unit	Maximum	Minimum	Mean	Median	Mode	Standard Deviation	Variance
Days	Day	28	7	17.5	17.5	7	10.5	110.6
Density	kg/m³	1400	800	1100	1100	800	223.9	50139.3
Percentage of eggshells	%	10.00	0.00	5.00	5.00	0.00	3.54	12.53
Water/cement ratio	-	0.64	0.56	0.60	0.60	0.56	0.03	0.00
Cement	kg/m³	547.0	331.0	430.9	423.0	346.0	76.5	5848.0
Sand	kg/m³	547.0	294.0	421.0	423.0	303.0	89.3	7979.2
Water	kg/m³	339.0	194.0	258.3	252.5	194.0	46.9	2198.3
Compressive Strength	MPa	8.69	0.53	3.05	2.05	1.23	2.18	4.74

(a) Days   (b) Density

(c) Percentage of Eggshells   (d) Water/cement Ratio

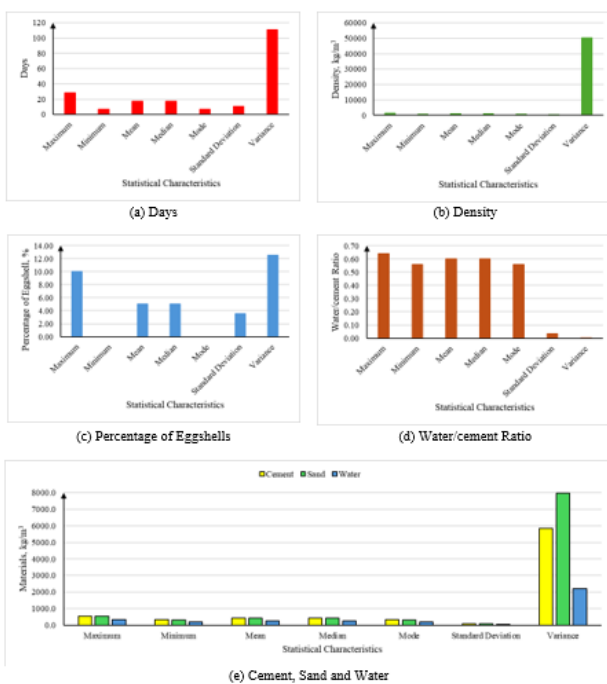(e) Cement, Sand and Water

Figure 2. Statistical Characteristics of Input Parameters
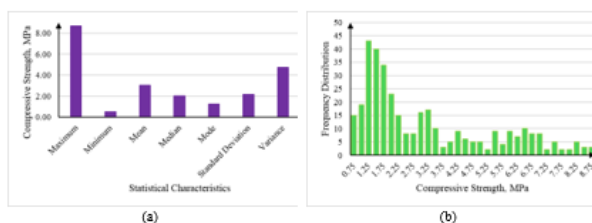

(a)   (b)

Figure 3. Statistical Characteristics of (a) Output Parameter and (b) Frequency Distribution of Output

This study further provides an analysis of the compressive strength data obtained from EFC samples with different densities, ranging from 800 kg/m³ to 1400 kg/m³, and tested over curing periods of 7 days and 28 days. The samples were mixed with eggshell replacement levels of 0%, 2.5%, 5%, 7.5%, and 10%, with mean compressive strengths measured by averaging the compressive strengths of three water/cement ratios of 0.56, 0.6, and 0.64, as shown in Table 3. A total of 360 experimental

samples were tested, and the results include mean compressive strength, standard deviation, maximum, and minimum compressive strengths for each density. At the lowest density of 800 kg/m³, the mean compressive strengths range from 0.67 MPa to 1.41 MPa (7 days) and 1.02 MPa to 1.80 MPa (28 days). As the density increases to 1000 kg/m³, the mean compressive strengths also increase, with values between 1.23 MPa to 1.51 MPa and 1.54 MPa to 1.79 MPa for the curing periods of 7-day and 28-day, respectively. At a density of 1200 kg/m³, the mean compressive strength improves further, ranging from 2.32 MPa to 2.97 MPa (7 days) and 3.05 MPa to 3.81 MPa (28 days). The 1400 kg/m³ density exhibits the most significant gain in compressive strength, with values ranging from 5.11 MPa to 5.83 MPa (7 days) and 6.62 MPa to 7.96 MPa (28 days).

These results show the substantial influence of density on the compressive strength of EFC, where higher densities consistently produce stronger concrete. The variability in compressive strength, as indicated by the standard deviation, also increases with density. For the 800 kg/m³ samples, the standard deviation ranges from 0.04 MPa to 0.11 MPa (7 days) and 0.04 MPa to 0.14 MPa (28 days), whereas for the 1400 kg/m³ samples, it increases to ranges of 0.47 MPa to 0.72 MPa (7 days) and 0.45 MPa to 0.87 MPa (28 days). This tendency implies that while compressive strength improves with density, there is also greater variability in the results for higher concrete density. Maximum and minimum compressive strengths similarly follow this trend, with the highest range of values recorded for the 1400 kg/m³ density. These findings emphasize the strong influence of density on both the compressive strength and the variability of eggshell foamed concrete.

Likewise, the influence of the water-to-cement ratio on compressive strength plays a significant role in the performance of eggshell foamed concrete based on the different densities, as shown in **Figure 4**. The influence of water/cement ratios on the 28-day compressive strength of eggshell foamed concrete becomes more pronounced as the density increases. At lower densities (800 kg/m³, 1000 kg/m³ and 1200 kg/m³), the w/c ratio has a relatively

minor effect on compressive strength. This indicates that at lower densities, the mix is more influenced by other factors such as the foamed structure or eggshell replacement percentage, with the cement content playing a less dominant role. However, as the density increases to 1400 kg/m³, the differences between the w/c ratios become more evident. In particular, the eggshell foamed concrete with a w/c ratio of 0.56 (red bars) achieved higher compressive strengths at 1400 kg/m³. Conversely, the w/c ratio of 0.64 (blue bars) shows a noticeable decline in strength at this density. This can be attributed to the higher water content, which weakens the eggshell foamed concrete by increasing porosity and reducing the bonding efficiency between the cement paste and the eggshell powers.

Table 3. Summary of Eggshell Foamed Concrete at Different Densities, Eggshell Replacements and Curing Ages

Density, kg/m³	Percentage of Eggshells, %	Days	Mean Compressive Strength, MPa	Standard Deviation, MPa	Maximum Compressive Strength, MPa	Minimum Compressive Strength, MPa
800	0	7	0.73	0.10	0.89	0.55
		28	1.02	0.14	1.22	0.87
	2.5	7	0.67	0.09	0.77	0.53
		28	1.14	0.07	1.25	1.03
	5	7	0.76	0.07	0.84	0.61
		28	1.20	0.08	1.28	1.01
	7.5	7	1.23	0.11	1.34	1.01
		28	1.70	0.04	1.74	1.60
	10	7	1.41	0.04	1.47	1.35
		28	1.80	0.09	1.91	1.67
1000	0	7	1.51	0.34	2.00	1.08
		28	1.79	0.39	2.42	1.23
	2.5	7	1.39	0.19	1.56	1.04
		28	1.69	0.25	2.22	1.46
	5	7	1.32	0.23	1.78	0.97
		28	1.60	0.30	2.01	1.25
	7.5	7	1.51	0.21	1.76	1.25
		28	1.54	0.33	1.89	1.09
	10	7	1.23	0.20	1.51	0.89
		28	1.70	0.44	2.16	0.98
1200	0	7	2.71	0.44	3.17	2.02
		28	3.64	0.49	4.23	3.00
	2.5	7	2.32	0.66	3.29	1.45
		28	3.05	0.85	4.26	2.27
	5	7	2.97	0.23	3.27	2.51
		28	3.56	0.56	4.29	2.88
	7.5	7	2.57	0.34	3.04	2.21
		28	3.81	0.68	4.61	2.77
	10	7	2.86	0.15	3.13	2.62
		28	3.64	0.31	3.98	3.13
1400	0	7	5.78	0.47	6.33	4.91
		28	7.96	0.72	8.69	6.77
	2.5	7	5.39	0.69	6.29	4.45
		28	7.28	0.87	8.42	6.31
	5	7	5.83	0.50	6.61	4.99
		28	7.39	0.64	8.36	6.55
	7.5	7	5.66	0.72	6.86	4.77
		28	6.81	0.64	7.75	5.74
	10	7	5.11	0.63	5.88	4.05
		28	6.62	0.45	7.36	5.98

2.4. Design of deep learning model

A deep learning model was designed to predict the compressive strength of EFC. **Figure 5** illustrates the architectural design of the deep learning model developed for this investigation, showcasing its various components and connections. The dataset utilized in this study comprised a total of 360 samples of EFC. The numerical input data encompassed crucial parameters, including the concrete age, density, eggshell replacement percentage, water/cement ratio as well as the weights assigned to

cement, sand, and water. Subsequently, an in-depth hyperparameter tuning process was conducted, systematically varying and assessing the number of hidden layers and neurons across multiple configurations, as detailed in Section 2.5. The output data was the compressive strength of the EFC.
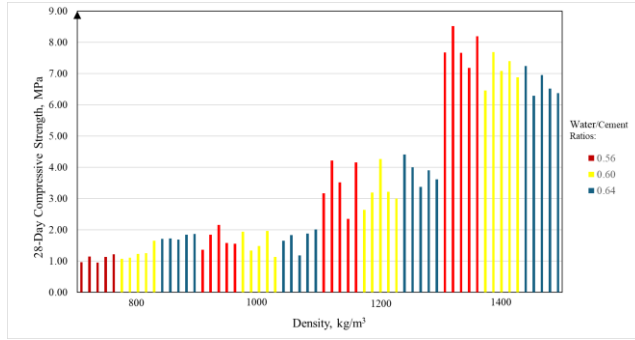

Figure 4. 28-Day Compressive Strength of Eggshell Foamed Concrete at Different Densities and Water/Cement Ratios (Note: Three colours are used to indicate the water/cement ratios of 0.56, 0.60, and 0.64, while each group of similarly coloured histograms consists of five columns to indicate different eggshell replacement levels from 0% to 10%.)
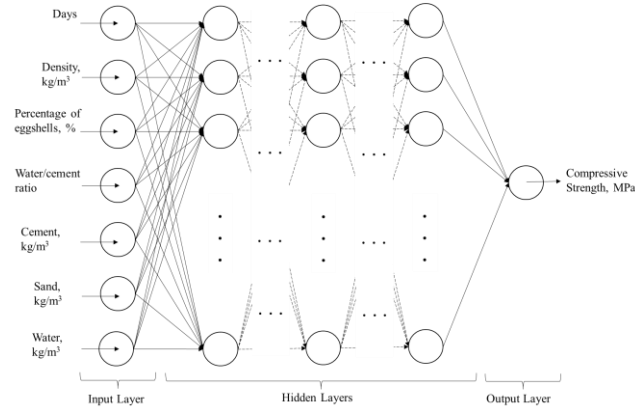

Figure 5. Design of Deep Neural Network Architecture

Before commencing the training phase, all numerical data underwent a normalization procedure to ensure uniform scaling, and the dataset was randomly shuffled to ensure the representativeness and randomness of the samples.

The dataset was divided into 70% for training, 15% for validation, and 15% for testing (see Table 4). The deep learning model was trained using the training dataset, validated with the validation dataset, and subsequently evaluated with the testing dataset to determine the model's performance. The main objective of this deep learning model was to deliver precise predictions of the compressive strength of EFC, leveraging the available input variables as the basis for robust inference. To facilitate the development of this model, Python programming and hyperparameter tuning were conducted using the Google Colaboratory platform.

2.5. Bayesian optimization for hyperparameter tuning

Bayesian optimization was employed as the methodology for hyperparameter tuning. Bayesian optimization is a powerful technique that enables efficient exploration of the hyperparameter space by iteratively evaluating the model performance and updating the search strategy based on the obtained results. It offers distinct advantages such as the ability to handle noisy and expensive-to-evaluate black-box functions, adaptability to various types of hyperparameters, and the ability to converge to the global optimum with limited evaluations (Candelieri, 2021). The objective of the optimization is to identify the highest value within a given sampling point for an unknown function f, as expressed by Equation 1 (Wu *et al.* 2019).

$$X^+ = arg arg\, f(X) \tag{1}$$

$$P(M|E) \propto P(M)P(M) \tag{2}$$

Bayesian optimization is rooted in Bayes' theorem, which states that the posterior probability P(M|E) of a model M, given evidence data E, is directly proportional to the likelihood P(E|M) of observing E given model M, multiplied by the prior probability P(M), as depicted in Equation 2 (Wu *et al.* 2019). Here, A represents the search space of X.

Table 4. Hyperparameters Tuning in the Deep Learning Model

Hyperparameter	Configuration
Data split (training: validation:test)	70%:15%:15%
Number of inputs	7
Number of hidden layers	1/2/3/4/5/6/7/8
Number of neurons	7/14/21/28/35
Number of outputs	1
Learning rate	0.01/0.001/0.0001
Activation function	Sigmoid/tanh/ReLU
Batch size	32
Optimizer	Adam
Epochs	100 to 1000 (increments of 100)

The specific configurations of the hyperparameters employed in the deep learning model as shown in Table 4. The hyperparameters tuning for Bayesian optimization encompassed the number of neurons, number of hidden layers, activation functions, and learning rate. The number

of neurons was explored across the values of 7, 14, 21, 28 and 35, while the number of hidden layers varied between 1, 2, 3, 4, 5, 6, 7 and 8. Different activation functions, including sigmoid, tanh, and ReLU, were investigated. The learning rate, a critical hyperparameter influencing the

speed and convergence of the model, was examined at values of 0.01, 0.001, and 0.0001. The training process was conducted for a fixed number of epochs (100), utilizing the Adam optimizer and a batch size of 32. After determining the optimal architecture for the deep learning model using Bayesian Optimization, subsequent hyperparameter tuning focused on varying the number of epochs. This was investigated across a range of values from 100 to 1000, in increments of 100. By exploring this diverse set of epoch values, the model's performance was further optimized.

2.6. Performance evaluation metrics

The performance of the deep learning model was evaluated through a comprehensive assessment of its hyperparameter tuning. The evaluation metrics employed for measuring the model's performance included the R-squared (R^2) coefficient of determination, Mean Squared Error (MSE) and Mean Absolute Error (MAE) (Harishkumar *et al.* 2020). The MSE was utilized as a metric to quantify the average squared difference between the predicted and actual values of the compressive strength (see Equation 3). It provides insight into the overall accuracy of the model's predictions, with lower MSE values indicating a closer fit to the true values. Likewise, the MAE was employed as an additional evaluation metric to measure the average absolute difference between the predicted and actual values (see Equation 4). This metric provides a measure of the model's precision and ability to capture the magnitude of the errors. Similar to MSE, lower MAE values signify better performance. Furthermore, the R^2 coefficient of determination was calculated to assess the goodness-of-fit of the model (see Equation 5). R^2 represents the proportion of the variance in the output variables that can be explained by the input variables. It ranges from 0 to 1, where a value closer to 1 indicates a stronger correlation and higher predictive power of the model (Huang *et al.* 2022).

$$MSE = \frac{1}{m} \sum_{i=1}^{m} \left(x_i - y_i \right)^2 \tag{3}$$

$$MAE = \frac{\sum_{i=1}^{m} \left| x_i - y_i \right|}{m} \tag{4}$$

$$R^2 = \frac{\sum_{i=1}^{m} \left(x_i - \underline{x}_i \right)\left(y_i - \underline{y}_i \right)}{\sqrt{\sum_{i=1}^{m} \left(x_i - \underline{x}_i \right)^2 \sum_{i=1}^{m} \left(y_i - \underline{y}_i \right)^2}} \tag{5}$$

Where m is the total number of samples, x_i and y_i are the actual and predicted values, $\bar{x}_i$ and $\bar{y}_i$ are the means of x_i and y_i (Ahmad *et al.* 2021).

Sensitivity analysis is a valuable tool for assessing a model's robustness by determining how uncertainties in inputs affect the output (Silva *et al.* 2023). It offers key insights into the relative importance of input parameters, helping researchers identify which factors most significantly influence the model results. Several recent studies have applied this technique. Silva *et al.* (2023) used sensitivity analysis to explore the relationship

between input variables and the mechanical properties of steel, providing a comprehensive assessment of each variable's impact on material behaviour. Liu *et al.* (2020) employed sensitivity analysis to evaluate the effect of input variables on frost durability in recycled aggregate concrete using soft computing methods. Similarly, Kumar *et al.* (2022) applied sensitivity analysis to identify key parameters affecting groundwater potential zones, revealing lithology as the most influential and soil type as the least. Overall, sensitivity analysis proves to be a robust and reliable method for examining the relative significance of model inputs.

In this study, a sensitivity analysis was conducted to assess the relative impact and importance of the input features on the output predictions of the developed deep learning model. Milne's method was employed to quantify the Relative Influence (RI) of the seven input parameters on the prediction of compressive strength. The RI was determined based on the magnitude of the connection weights between the neural networks within the model. Equation 6 was utilized to calculate the RI, providing a comprehensive measure of the contribution of each input feature to the prediction accuracy of the model (Getahun *et al.* 2018).

$$RI = \frac{\sum_{j=1}^{n_{hid}} \frac{w_{ji}}{\sum_{l=1}^{n_{inp}} \left| w_{jl} \right|} \times w_{oj}}{\sum_{k=1}^{n_{inp}} \left(\sum_{j=1}^{n_{hid}} \left| \frac{w_{jk}}{\sum_{l=1}^{n_{inp}} \left| w_{jl} \right|} \times w_{oj} \right| \right)} \times 100\% \tag{6}$$

Where n_{inp} and n_{hid} are the numbers of input and hidden layers, w is the weight of connection, i and o are the input and output units.

3.   Results and discussion

3.1. Best-performing deep learning infrastructure

Bayesian optimization was used to fine-tune the hyperparameters of the deep learning model for predicting the compressive strength of EFC. This optimization process successfully identified the optimal set of hyperparameters, resulting in the best-performing model. The optimized hyperparameters included an input layer with 7 units, indicating the number of features used as input for the model. Four hidden layers were employed with the layers consisting of 28, 21, 28 and 21 neurons. The ReLU activation function was applied to these neurons, renowned for its effectiveness in handling non-linearity and mitigating the vanishing gradient problem (Hu *et al.* 2021). This contributed to the model's improved performance by facilitating the efficient propagation of information through the network. Additionally, a learning rate of 0.01 was chosen to determine the step size for adjusting the model's parameters during the training process. The selection of these hyperparameters was based on their ability to maximize the predictive performance of the model. By striking the right balance between the number of hidden layers, the number of neurons, and the learning rate, the model achieved a high

level of accuracy in predicting the compressive strength of EFC.

To determine the optimal number of epochs for training the deep learning model, an investigation was conducted where the number of epochs was varied from 100 to 1000 in increments of 100. The performance of the model was evaluated based on metrics as shown in Table 5, such as the MAE, MSE and R^2 values. The results of the investigation revealed that the model achieved its best performance when trained for 200 epochs. The model trained for 200 epochs exhibited a MAE of 0.0.0382, with a range of values in the investigated epochs ranging from 0.0382 to 0.0483. The MSE for the 200-epoch model was

0.0522, within the range of 0.0522 to 0.0723 observed across the investigated epochs. Additionally, the R^2 value for the 200-epoch model was 0.9548, which fell within the range of 0.9256 to 0.9548 observed throughout the investigation. The selection of 200 epochs as the optimal number was based on achieving the lowest values for MAE and MSE, along with the highest R^2 value (Huang *et al.* 2022). These metrics indicate the model's accuracy, precision, and fit quality. The results show that the model's predictive performance improved with an increase in the number of epochs up to 200, beyond which further training offered diminishing returns.

Table 5. Evaluation Performance of Different Numbers of Epochs

Evaluation	Epochs									
	100	200	300	400	500	600	700	800	900	1000
MAE	0.0450	0.0382	0.0436	0.0418	0.0477	0.0477	0.0483	0.0472	0.0472	0.0469
MSE	0.0613	0.0522	0.0641	0.0658	0.0667	0.0624	0.0692	0.0718	0.0723	0.0682
R^2	0.9466	0.9548	0.9415	0.9390	0.9409	0.9449	0.9319	0.9290	0.9256	0.9336

In this study, the utilization of Bayesian optimization in developing the deep learning model contributes significantly to the concrete properties' prediction field. It enhances the predictive accuracy of the model by efficiently exploring the hyperparameter space and identifying the optimal hyperparameter settings (Turner *et al.* 2021). This optimization process leads to the selection of hyperparameter configurations that minimize errors to ensure the model's ability to accurately predict the compressive strength of EFC. It facilitates efficient model training, addressing the resource-intensive nature of deep learning models. By narrowing down the search space for optimal hyperparameters, the computational burden and time required for model training are significantly reduced (Snoek *et al.* 2012). This efficiency not only expedites the research process but also enables the scalability of the deep learning model. Researchers can easily apply the developed model to larger datasets or extend its applicability to other concrete research studies, improving the overall productivity and effectiveness of the field.

3.2. Learning curve for the best-performing model

The learning curve was plotted to explore in more detail the training process of the best-performing model, which was trained for 200 epochs. The learning curve, depicted in **Figure 6**, showcased the relationship between the loss values (MSE) and the number of epochs. The curve encompassed two distinct lines, such as the training loss line represented in red and the validation loss line represented in blue. Both the training and validation loss lines displayed a similar trend throughout the training process. Initially, at the early stages of training, both lines exhibited higher loss values, indicating the model's inability to accurately predict the compressive strength of the EFC. However, as the training progressed, the loss values decreased, suggesting that the model was effectively learning from the training data and making improvements in its predictive capabilities (Tsehay *et al.*

2017). As the number of epochs increased, both the training and validation loss lines reached a plateau, indicating that the model had trained to a stable state.
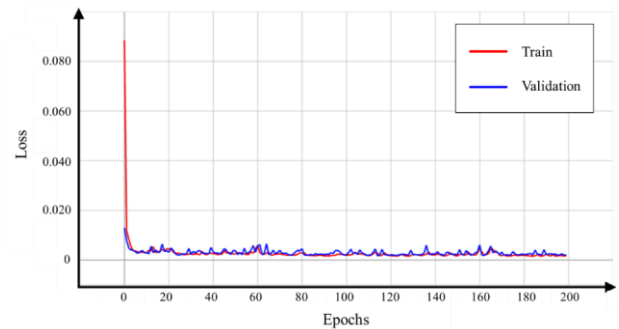
Figure 6. Learning Curve for the Best Performance Model with 200 Epochs

3.3. Regression analysis for the predicted and testing datasets

Regression analysis was conducted to assess the performance of the top-performing model in predicting the compressive strength of EFC. The results of the regression analysis are presented in **Figure 7**, which showcases the relationship between the predicted and testing datasets. The scatter plot visually represents the testing data points as blue dots, while the regression line is depicted in red. The equation of the regression line, y = 0.97x + 0.03, highlights a strong positive correlation between the predicted and testing datasets. Notably, the regression line closely aligns with the data points, indicating the model's ability to provide accurate estimations of the compressive strength. This regression analysis provides additional evidence, further reinforcing the reliability of the developed deep learning model in accurately predicting the compressive strength of EFC. Accurate prediction of compressive strength in EFC plays a crucial role in ensuring effective quality control throughout the production process. By employing a reliable predictive model, manufacturers can confidently

verify that the concrete meets the desired strength requirements and exhibits the expected density. This level of control and consistency in construction materials is essential for minimizing the risk of structural failures and ensuring the durability of built structures (Magudeaswaran *et al.* 2020).
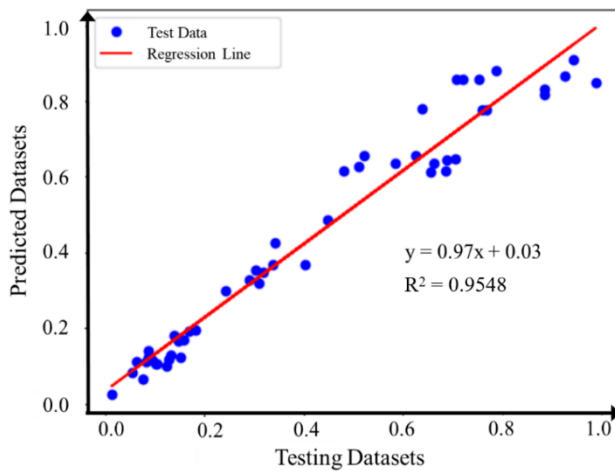
Figure 7. Regression Analysis for the Best-Performing Model

3.4. Sensitivity analysis

To gain insights into the relative influence of input features on the output, a sensitivity analysis was conducted using Milne's method to calculate the RI. The RI values were then converted to percentages to provide a clearer understanding of the impact of each input feature on the compressive strength of EFC. **Figure 8** illustrates the RI percentages of the input features on the compressive strength. The results of the sensitivity analysis revealed that the water/cement ratio had the highest RI, accounting for 31% of the variation in compressive strength. This suggests that the water-to-cement ratio plays a significant role in determining the strength of the concrete. Following closely, the amount of sand in the mixture exhibited RI of 26%, highlighting its importance in influencing compressive strength. Cement content contributed to 14% of the variation, while water content and the number of days of curing each accounted for 7% of the overall influence. The density of the concrete exhibited a RI of 9%. Surprisingly, the percentage of eggshell replacement had a relatively lower influence at 6%.

The observed percentages in the sensitivity analysis shed light on the critical factors that affect the compressive strength of EFC. The significant influence of the water/cement ratio highlights the importance of maintaining an appropriate balance in the mix design. Consistent with Zhao *et al.* (2018) and Retamal and Rougier (2021), the water/cement ratio was identified as the most influential factor, highlighting the necessity of carefully controlling this parameter to achieve desired strength levels. The high influence of sand suggests its role in providing structural integrity and stability to the concrete. Cement content directly affects the binding properties and contributes to the overall strength. Nevertheless, the relatively lower influence of the eggshell replacement percentage observed in this study

contradicts the findings of Ghahremani *et al.* (2023), highlighting the need for further investigation into the role of eggshell content in predicting the compressive strength of foamed concrete. Despite its lower impact, the inclusion of eggshells in the mix design remains significant due to its potential for enhancing sustainability and waste utilization. Overall, the sensitivity analysis provides valuable insights into the relative importance of different input features on the compressive strength of EFC.
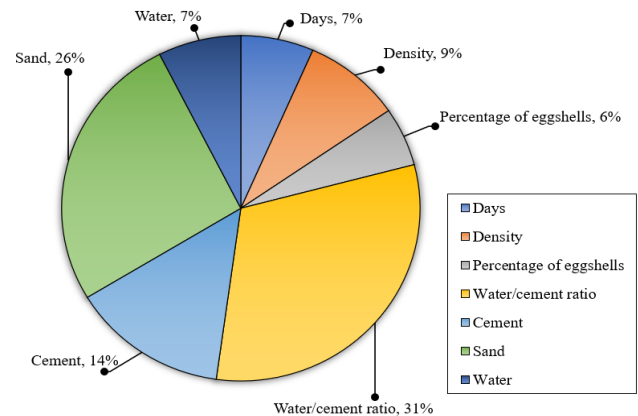
Figure 8. Relative Influence Percentages of Input Features on the Outputs

4. Conclusions

This study successfully developed and optimized a deep learning model for predicting the compressive strength of eggshell-based foamed concrete. The key findings are as follows:

- The best-performing model, identified through Bayesian optimization, has four hidden layers with 28, 21, 28 and 21 neurons and ReLU activation functions.

- The model was trained with a learning rate of 0.01, achieving high predictive accuracy.

- Optimal performance was observed with 200 epochs, showcasing the lowest MSE and MAE, as well as the highest R2 value.

- Learning curve analysis indicated the model's ability to generalize without overfitting or underfitting.

- Regression analysis showed a strong positive correlation between predicted and actual compressive strength, confirming the model's accuracy.

- Sensitivity analysis revealed that the water/cement ratio had the highest influence on compressive strength, accounting for 31% of the variation. The percentage of eggshell replacement had a lower impact but is important for sustainability and waste utilization.

Overall, the developed deep learning model contributes significantly to the field of construction materials by providing a robust and reliable tool for accurately predicting the compressive strength of eggshell-based foamed concrete. The insights from the sensitivity analysis

guide future efforts in mix design optimization and quality control. Last but not least, the integration of advanced prediction models based on deep learning not only enhances the understanding of concrete properties but also paves the way for transformative changes in construction practices. By leveraging the power of data-driven modelling and optimization techniques, researchers can drive innovation, improve decision-making processes, and ultimately contribute to the sustainable development of the construction industry. The accurate prediction of compressive strength in eggshell-based foamed concrete is a critical step towards achieving these goals, as it empowers engineers and stakeholders to make informed choices that lead to safer, more efficient, and environmentally conscious construction practices. Future research may further explore the applicability of the developed model to different concrete compositions and expand its capabilities to include other concrete properties of interest.

Acknowledgements

References

Ahmad A., Farooq F., Niewiadomski P., Ostrowski K., Akbar A., Aslam F. and Alyousef R. (2021). Prediction of compressive strength of fly ash based concrete using individual and ensemble algorithm, *Materials*, **14(4)**, 794.

Ali T., El Ouni M.H., Qureshi M.Z., Islam A.B.M.S., Mahmood M.S., Ahmed H. and Ajwad A. (2024). A systematic literature review of AI-based prediction methods for self-compacting, geopolymer, and other eco-friendly concrete types: Advancing sustainable concrete, Construction and Building Materials, **440**, 137370

ASTM (2012), Standard Specification for Portland Cement (ASTM C150), American Society for Testing and Materials, West Conshohocken, Pennsylvania: ASTM International.

ASTM (2021), Standard Specification for Standard Sand (ASTM C778), American Society for Testing and Materials, West Conshohocken, Pennsylvania: ASTM International.

ASTM (2023), Standard Specification for Concrete Aggregates (ASTM C33), American Society for Testing and Materials, West Conshohocken, Pennsylvania: ASTM International.

BSI (2013), Aggregates for Concrete (BS EN 12620), British Standards Institution, London.

BSI, (2002), BS EN 12390-3: Testing hardened concrete, Part 3: Compressive strength of test specimens, British Standard Institute.

Candelieri A. (2021). A gentle introduction to Bayesian optimization, In: 2021 Winter Simulation Conference (WSC), 1–16.

de-Prado-Gil J., Zaid O., Palencia C. and Martínez-García R. (2022). Prediction of splitting tensile strength of self-compacting recycled aggregate concrete using novel deep learning methods, *Mathematics*, **10(13)**, 2245.

DSM (2014), Cement - Part 1: Composition, specifications and conformity criteria for common cements (MS EN 197-1), Department of Standards Malaysia.

Falah M.W., Hussein S.H., Saad M.A., Ali Z.H., Tran T.H., Ghoniem R.M. and Ewees A.A. (2022), Compressive strength prediction using coupled deep learning model with extreme gradient boosting algorithm: Environmentally friendly concrete incorporating recycled aggregate, *Complexity*, **2022**, 5433474:1-5433474:22.

Falliano D., De Domenico D., Ricciardi G. and Gugliandolo E. (2018), Key factors affecting the compressive strength of foamed concrete, *IOP Conference Series: Materials Science and Engineering*, **431**.

Gao Y. and Ma R. (2024), A Comparative Study of Machine Learning and Conventional Techniques in Predicting Compressive Strength of Concrete with Eggshell and Glass Powder Additives, *Buildings*, **14(9)**, 2956.

Getahun M.A., Shitote S.M. and Gariy Z.C.A. (2018), Artificial neural network based modelling approach for strength prediction of concrete incorporating agricultural and construction wastes, *Construction and Building Materials*, **190**, 517–525.

Ghahremani G., Bagheri A. and Zanganeh H. (2023), The effect of size and shape of pores on the prediction model of compressive strength of foamed concrete, *Construction and Building Materials*, **371**, 130720.

Hafiz M.M.A., Ridzuan A.R.M., Fadzil M.A. and Nurliza J. (2014), Chemical characterization of used cooking oil foaming agent as admixture in foamed concrete, In: *InCIEC 2013: Proceedings of the International Civil and Infrastructure Engineering Conference 2013*, 191–200.

Harishkumar K.S., Yogesh K.M. and Gad I. (2020), Forecasting air pollution particulate matter (PM2.5) using machine learning regression models, *Procedia Computer Science*, **171**, 2057–2066.

Hu Z., Zhang J. and Ge Y. (2021), Handling vanishing gradient problem using artificial derivative, *IEEE Access*, **9**, 22371–22377.

Huang X.Y., Wu K.Y., Wang S., Lu T., Lu Y.F., Deng W.C. and Li H.M. (2022), Compressive strength prediction of rubber concrete based on artificial neural network model with hybrid particle swarm optimization algorithm, *Materials*, **15(11)**, 3934.

Jhatial A.A., Goh W.I., Kumar R., Siddiqui F.H., Kamaruddin S. and Rahman A.F. (2021a), Flexural behaviour, microstructure and cost-benefit analysis of ternary binder foamed concrete, *Journal of Engineering Research*, **10(2B)**, 1–27.

Jhatial A.A., Goh W.I., Mohamad N., Mo K.H. and Mehroz A. (2021b), Thermomechanical evaluation of sustainable foamed concrete incorporating palm oil fuel ash and eggshell powder, *Journal of Engineering Research*, **9(3A)**, 64–79.

Jhatial A.A., Goh W.I., Sohu S., Mangi S.A. and Mastoi A.K. (2020), Preliminary investigation of thermal behavior of lightweight foamed concrete incorporating palm oil fuel ash and eggshell powder, *Periodica Polytechnica Civil Engineering*, **65(1)**, 168–180.

Kavya K.S., Jithiya K.K., Athulya Vijay N., Jayan J.L., Karthik M., Sheela Evangeline Y. and Jose S.K. (2020), Study on the effect of soil as a filler in foamed concrete, In: *Construction in Geotechnical Engineering: Proceedings of IGC 2018*, 17–25.

Khan K., Ahmad W., Amin M.N. and Deifalla A.F. (2023), Investigating the feasibility of using waste eggshells in cement-based materials for sustainable construction, *Journal of Materials Research and Technology*, **23**, 4059–4074.

Kumar M., Singh S.K., Kundu A., Tyagi K., Menon J., Frederick A., Raj A. and Lal D., (2022), GIS-based multi-criteria approach to delineate groundwater prospect zone and its sensitivity analysis, *Applied Water Science*, **12(4)**, 71.

Lim S.K., Foo K.P., Lee F.W., Tiong H.Y., Lee Y.L., Lim J.H. and King Y.J. (2021). Acoustic properties of lightweight foamed concrete with eggshell waste as partial cement replacement material, *Sains Malaysiana*, **50**, 537–547.

Lim S.K., Tan C.S., Zhao X. and Ling T.C. (2015). Strength and toughness of lightweight foamed concrete with different sand grading, *KSCE Journal of Civil Engineering*, **19**, 2191–2197.

Liu K., Zou C., Zhang X. and Yan J. (2021). Innovative prediction models for the frost durability of recycled aggregate concrete using soft computing methods, *Journal of Building Engineering*, **34**, 101822.

Liu M.Y.J., Alengaram U.J., Yap S.P. and Jumaat M.Z. (2014). Utilization of oil palm shell as lightweight aggregate in lightweight-foamed concrete, *Australian Journal of Basic and Applied Sciences*, **8(19)**, 119–122.

Magudeaswaran P., Kumar C.V. and Ravinder R. (2020). Prediction of strength and durability properties of HPC composites using Adaptive Neuro-fuzzy Inference System, *E3S Web of Conferences*, **184**, 01102.

Mahmood M.S., Elahi A., Zaid O., Alashker Y., Şerbănoiu A.A., Grădinaru C.M., Ullah K. and Ali T. (2023). Enhancing compressive strength prediction in self-compacting concrete using machine learning and deep learning techniques with incorporation of rice husk ash and marble powder, *Case Studies in Construction Materials*, **19**, e02557.

Mydin M.A.O. (2023). Engineering properties of lightweight foamed concrete strengthen with fibreglass netting, *Jurnal Teknologi*, **85(3)**, 165–173.

Mydin M.A.O., Nawi M. and Salameh A. (2022). Mechanical properties of low densities lightweight foamed concrete strengthen with raw empty fruit bunch fibre, *Tehnički Vjesnik - Technical Gazette*, **29(2)**, 646–651.

Othman R., Putra Jaya R., Duraisamy Y., Sulaiman M.A., Chong B.W. and Ghamari A. (2023). Efficiency of waste as cement replacement in foamed concrete—A review, *Sustainability*, **15(6)**, 5163.

Pirah J.A., Mydin M.A.O., Khalid M.S. and Omar R. (2022). Application of alkali-resistant woven fibre mesh confinement to strengthen lightweight foamed concrete, *Journal of Advanced Research in Applied Sciences and Engineering Technology*, **29(1)**, 101–109.

Rahman A.F., Goh W.I. and Jhatial A.A. (2019). Flexural study of reinforced foamed concrete beam containing palm oil fuel ash (POFA) and eggshell powder (ESP) as partial cement replacement, *International Journal of Sustainable Construction Engineering and Technology*, **10(1)**, 93–100.

Rahman A.F., Goh W.I., Othman N.H. and Kamaruddin M.S. (2021). Study on mechanical properties of foamed concrete incorporating palm oil fuel ash and mussel shell as partial cement replacement, *IOP Conference Series: Materials Science and Engineering*, **1200(1)**, 012005.

Retamal F.A. and Rougier V.C. (2021). Calibration of a strength prediction model for foamed cellular concrete, In: *Proceedings of the 19th LACCEI International Multi-Conference for Engineering, Education, and Technology*, 1–7.

Serudin A.M., Mydin M.A.O. and Abdul Ghani A.N. (2022). Investigating the load carrying capacities of lightweight foamed concrete strengthen with fiber mesh, *International Journal of Integrated Engineering*, **14(4)**, 360–376.

Shah S.N., Mo K.H., Yap S.P., Yang J. and Ling T.C. (2021). Lightweight foamed concrete as a promising avenue for incorporating waste materials: A review, Resources, *Conservation & Recycling*, **164**, 105103.

Sharafati A., Naderpour H., Salih S.Q., Onyari E.K. and Yaseen Z.M. (2021). Simulation of foamed concrete compressive strength prediction using adaptive neuro-fuzzy inference system optimized by nature-inspired algorithms, *Frontiers of Structural and Civil Engineering*, **15**, 61–79.

Silva K.R., Serpa P., Sgrott D.M., Cerqueira F.M., Miranda F., Silva F.J.F. and Parpinelli R.S. (2023). Ensemble of artificial neural networks and AutoML for predicting steel properties, In *Proceedings of the Anais do XVI Congresso Brasileiro de Inteligência Computacional (CBIC 2023)*, Salvador, Brazil, 8–11 October 2023.

Singh P., Bhardwaj S., Bera P., Lone T., Karim S. and Singh S.K. (2021). Development of forecasting model for prediction of compressive strength of foamed concrete using density with W/C ratio and S/C ratio by the application of ANN, *IOP Conference Series: Earth and Environmental Science*, **889**, 012039

Snoek J., Larochelle H. and Adams R.P. (2012), Practical Bayesian optimization of machine learning algorithms, *Advances in Neural Information Processing Systems*, **25**.

Suhaili S.S., Alias N.N., Mydin M.A.O. and Awang H. (2021), Influence of oil palm spikelets fibre on mechanical properties of lightweight foamed concrete, *Journal of Civil Engineering Science and Technology*, **12(2)**, 160–167.

Sumiati M. and Sukarman S. (2020). The utilization of crushed clay brick as coarse aggregate on eco-green lightweight foamed concrete, *Journal of Physics: Conference Series*, **1500**, 012070.

Tiong H.Y., Lim S.K. and Lee Y.L. (2022). Dimensional stability of lightweight foamed concrete containing eggshell powder and calcium stearate, *International Journal of Integrated Engineering*, **14(1)**, 260–268.

Tiong H.Y., Lim S.K., Lee Y.L. and Lim J.H. (2018). Engineering properties of 1200 kg/m³ lightweight foamed concrete with eggshell powder as partial replacement material of cement, *E3S Web of Conferences*, **65**, 02010.

Tsehay Y.K., Lay N.S., Roth H.R., Wang X., Kwak J.T., Turkbey B.I. and Summers R.M. (2017). Convolutional neural network-based deep-learning architecture for prostate cancer detection on multiparametric magnetic resonance images, In: Medical Imaging 2017: *Computer-Aided Diagnosis*, **10134**, 20–30.

Turner R., Eriksson D., McCourt M., Kiili J., Laaksonen E., Xu Z. and Guyon I. (2021). Bayesian optimization is superior to random search for machine learning hyperparameter tuning: Analysis of the black-box optimization challenge 2020, In: *NeurIPS 2020 Competition and Demonstration Track*, 3–26.

Villiers D. and Petrus J. (2016). Bond of deformed steel reinforcement in lightweight foamed concrete, *Structural Concrete*, **18(3)**, 496–506.

Wong S.H., Shek P.N., Saggaff A., Tahir M.M. and Lee Y.H. (2019). Compressive strength prediction of lightweight foamed concrete with various densities, *IOP Conference Series: Materials Science and Engineering*, **620**, 012043

Wu J., Chen X.Y., Zhang H., Xiong L.D., Lei H. and Deng S.H. (2019). Hyperparameter optimization for machine learning

models based on Bayesian optimization, *Journal of Electronic Science and Technology*, **17(1)**, 26–40.

Zhao W.H., Huang J., Su Q. and Liu T.L. (2018). Models for strength prediction of high-porosity cast-in-situ foamed concrete, *Advances in Materials Science and Engineering*, 2018, 1–10.

Supplementary Data: Mix Design

Day	Density, kg/m³	Eggshell replacement, %	Water/cement Ratios	Cement, kg/m³	Sand, kg/m³	Water, kg/m³
7	800	0	0.56	346	303	194
7	800	0	0.56	346	303	194
7	800	0	0.56	346	303	194
28	800	0	0.56	346	303	194
28	800	0	0.56	346	303	194
28	800	0	0.56	346	303	194
7	800	0	0.6	338	299	203
7	800	0	0.6	338	299	203
7	800	0	0.6	338	299	203
28	800	0	0.6	338	299	203
28	800	0	0.6	338	299	203
28	800	0	0.6	338	299	203
7	800	0	0.64	331	294	212
7	800	0	0.64	331	294	212
7	800	0	0.64	331	294	212
28	800	0	0.64	331	294	212
28	800	0	0.64	331	294	212
28	800	0	0.64	331	294	212
7	800	2.5	0.56	346	303	194
7	800	2.5	0.56	346	303	194
7	800	2.5	0.56	346	303	194
28	800	2.5	0.56	346	303	194
28	800	2.5	0.56	346	303	194
28	800	2.5	0.56	346	303	194
7	800	2.5	0.6	338	299	203
7	800	2.5	0.6	338	299	203
7	800	2.5	0.6	338	299	203
28	800	2.5	0.6	338	299	203
28	800	2.5	0.6	338	299	203
28	800	2.5	0.6	338	299	203
7	800	2.5	0.64	331	294	212
7	800	2.5	0.64	331	294	212
7	800	2.5	0.64	331	294	212
28	800	2.5	0.64	331	294	212
28	800	2.5	0.64	331	294	212
28	800	2.5	0.64	331	294	212
7	800	5	0.56	346	303	194
7	800	5	0.56	346	303	194
7	800	5	0.56	346	303	194
28	800	5	0.56	346	303	194
28	800	5	0.56	346	303	194
28	800	5	0.56	346	303	194
7	800	5	0.6	338	299	203
7	800	5	0.6	338	299	203
7	800	5	0.6	338	299	203
28	800	5	0.6	338	299	203
28	800	5	0.6	338	299	203

28	800	5	0.6	338	299	203
7	800	5	0.64	331	294	212
7	800	5	0.64	331	294	212
7	800	5	0.64	331	294	212
28	800	5	0.64	331	294	212
28	800	5	0.64	331	294	212
28	800	5	0.64	331	294	212
7	800	7.5	0.56	346	303	194
7	800	7.5	0.56	346	303	194
7	800	7.5	0.56	346	303	194
28	800	7.5	0.56	346	303	194
28	800	7.5	0.56	346	303	194
28	800	7.5	0.56	346	303	194
7	800	7.5	0.6	338	299	203
7	800	7.5	0.6	338	299	203
7	800	7.5	0.6	338	299	203
28	800	7.5	0.6	338	299	203
28	800	7.5	0.6	338	299	203
28	800	7.5	0.6	338	299	203
7	800	7.5	0.64	331	294	212
7	800	7.5	0.64	331	294	212
7	800	7.5	0.64	331	294	212
28	800	7.5	0.64	331	294	212
28	800	7.5	0.64	331	294	212
28	800	7.5	0.64	331	294	212
7	800	10	0.56	346	303	194
7	800	10	0.56	346	303	194
7	800	10	0.56	346	303	194
28	800	10	0.56	346	303	194
28	800	10	0.56	346	303	194
28	800	10	0.56	346	303	194
7	800	10	0.6	338	299	203
7	800	10	0.6	338	299	203
7	800	10	0.6	338	299	203
28	800	10	0.6	338	299	203
28	800	10	0.6	338	299	203
28	800	10	0.6	338	299	203
7	800	10	0.64	331	294	212
7	800	10	0.64	331	294	212
7	800	10	0.64	331	294	212
28	800	10	0.64	331	294	212
28	800	10	0.64	331	294	212
28	800	10	0.64	331	294	212
7	1000	0	0.56	391	391	219
7	1000	0	0.56	391	391	219
7	1000	0	0.56	391	391	219
28	1000	0	0.56	391	391	219
28	1000	0	0.56	391	391	219
28	1000	0	0.56	391	391	219
7	1000	0	0.6	385	385	231
7	1000	0	0.6	385	385	231
7	1000	0	0.6	385	385	231
28	1000	0	0.6	385	385	231
28	1000	0	0.6	385	385	231
28	1000	0	0.6	385	385	231
7	1000	0	0.64	379	379	242
7	1000	0	0.64	379	379	242
7	1000	0	0.64	379	379	242
28	1000	0	0.64	379	379	242

28	1000	0	0.64	379	379	242
28	1000	0	0.64	379	379	242
7	1000	2.5	0.56	391	391	219
7	1000	2.5	0.56	391	391	219
7	1000	2.5	0.56	391	391	219
28	1000	2.5	0.56	391	391	219
28	1000	2.5	0.56	391	391	219
28	1000	2.5	0.56	391	391	219
7	1000	2.5	0.6	385	385	231
7	1000	2.5	0.6	385	385	231
7	1000	2.5	0.6	385	385	231
28	1000	2.5	0.6	385	385	231
28	1000	2.5	0.6	385	385	231
28	1000	2.5	0.6	385	385	231
7	1000	2.5	0.64	379	379	242
7	1000	2.5	0.64	379	379	242
7	1000	2.5	0.64	379	379	242
28	1000	2.5	0.64	379	379	242
28	1000	2.5	0.64	379	379	242
28	1000	2.5	0.64	379	379	242
7	1000	5	0.56	391	391	219
7	1000	5	0.56	391	391	219
7	1000	5	0.56	391	391	219
28	1000	5	0.56	391	391	219
28	1000	5	0.56	391	391	219
28	1000	5	0.56	391	391	219
7	1000	5	0.6	385	385	231
7	1000	5	0.6	385	385	231
7	1000	5	0.6	385	385	231
28	1000	5	0.6	385	385	231
28	1000	5	0.6	385	385	231
28	1000	5	0.6	385	385	231
7	1000	5	0.64	379	379	242
7	1000	5	0.64	379	379	242
7	1000	5	0.64	379	379	242
28	1000	5	0.64	379	379	242
28	1000	5	0.64	379	379	242
28	1000	5	0.64	379	379	242
7	1000	7.5	0.56	391	391	219
7	1000	7.5	0.56	391	391	219
7	1000	7.5	0.56	391	391	219
28	1000	7.5	0.56	391	391	219
28	1000	7.5	0.56	391	391	219
28	1000	7.5	0.56	391	391	219
7	1000	7.5	0.6	385	385	231
7	1000	7.5	0.6	385	385	231
7	1000	7.5	0.6	385	385	231
28	1000	7.5	0.6	385	385	231
28	1000	7.5	0.6	385	385	231
28	1000	7.5	0.6	385	385	231
7	1000	7.5	0.64	379	379	242
7	1000	7.5	0.64	379	379	242
7	1000	7.5	0.64	379	379	242
28	1000	7.5	0.64	379	379	242
28	1000	7.5	0.64	379	379	242
28	1000	7.5	0.64	379	379	242
7	1000	10	0.56	391	391	219
7	1000	10	0.56	391	391	219
7	1000	10	0.56	391	391	219

28	1000	10	0.56	391	391	219
28	1000	10	0.56	391	391	219
28	1000	10	0.56	391	391	219
7	1000	10	0.6	385	385	231
7	1000	10	0.6	385	385	231
7	1000	10	0.6	385	385	231
28	1000	10	0.6	385	385	231
28	1000	10	0.6	385	385	231
28	1000	10	0.6	385	385	231
7	1000	10	0.64	379	379	242
7	1000	10	0.64	379	379	242
7	1000	10	0.64	379	379	242
28	1000	10	0.64	379	379	242
28	1000	10	0.64	379	379	242
28	1000	10	0.64	379	379	242
7	1200	0	0.56	469	469	263
7	1200	0	0.56	469	469	263
7	1200	0	0.56	469	469	263
28	1200	0	0.56	469	469	263
28	1200	0	0.56	469	469	263
28	1200	0	0.56	469	469	263
7	1200	0	0.6	462	462	277
7	1200	0	0.6	462	462	277
7	1200	0	0.6	462	462	277
28	1200	0	0.6	462	462	277
28	1200	0	0.6	462	462	277
28	1200	0	0.6	462	462	277
7	1200	0	0.64	455	455	291
7	1200	0	0.64	455	455	291
7	1200	0	0.64	455	455	291
28	1200	0	0.64	455	455	291
28	1200	0	0.64	455	455	291
28	1200	0	0.64	455	455	291
7	1200	2.5	0.56	469	469	263
7	1200	2.5	0.56	469	469	263
7	1200	2.5	0.56	469	469	263
28	1200	2.5	0.56	469	469	263
28	1200	2.5	0.56	469	469	263
28	1200	2.5	0.56	469	469	263
7	1200	2.5	0.6	462	462	277
7	1200	2.5	0.6	462	462	277
7	1200	2.5	0.6	462	462	277
28	1200	2.5	0.6	462	462	277
28	1200	2.5	0.6	462	462	277
28	1200	2.5	0.6	462	462	277
7	1200	2.5	0.64	455	455	291
7	1200	2.5	0.64	455	455	291
7	1200	2.5	0.64	455	455	291
28	1200	2.5	0.64	455	455	291
28	1200	2.5	0.64	455	455	291
28	1200	2.5	0.64	455	455	291
7	1200	5	0.56	469	469	263
7	1200	5	0.56	469	469	263
7	1200	5	0.56	469	469	263
28	1200	5	0.56	469	469	263
28	1200	5	0.56	469	469	263
28	1200	5	0.56	469	469	263
7	1200	5	0.6	462	462	277
7	1200	5	0.6	462	462	277

7	1200	5	0.6	462	462	277
28	1200	5	0.6	462	462	277
28	1200	5	0.6	462	462	277
28	1200	5	0.6	462	462	277
7	1200	5	0.64	455	455	291
7	1200	5	0.64	455	455	291
7	1200	5	0.64	455	455	291
28	1200	5	0.64	455	455	291
28	1200	5	0.64	455	455	291
28	1200	5	0.64	455	455	291
7	1200	7.5	0.56	469	469	263
7	1200	7.5	0.56	469	469	263
7	1200	7.5	0.56	469	469	263
28	1200	7.5	0.56	469	469	263
28	1200	7.5	0.56	469	469	263
28	1200	7.5	0.56	469	469	263
7	1200	7.5	0.6	462	462	277
7	1200	7.5	0.6	462	462	277
7	1200	7.5	0.6	462	462	277
28	1200	7.5	0.6	462	462	277
28	1200	7.5	0.6	462	462	277
28	1200	7.5	0.6	462	462	277
7	1200	7.5	0.64	455	455	291
7	1200	7.5	0.64	455	455	291
7	1200	7.5	0.64	455	455	291
28	1200	7.5	0.64	455	455	291
28	1200	7.5	0.64	455	455	291
28	1200	7.5	0.64	455	455	291
7	1200	10	0.56	469	469	263
7	1200	10	0.56	469	469	263
7	1200	10	0.56	469	469	263
28	1200	10	0.56	469	469	263
28	1200	10	0.56	469	469	263
28	1200	10	0.56	469	469	263
7	1200	10	0.6	462	462	277
7	1200	10	0.6	462	462	277
7	1200	10	0.6	462	462	277
28	1200	10	0.6	462	462	277
28	1200	10	0.6	462	462	277
28	1200	10	0.6	462	462	277
7	1200	10	0.64	455	455	291
7	1200	10	0.64	455	455	291
7	1200	10	0.64	455	455	291
28	1200	10	0.64	455	455	291
28	1200	10	0.64	455	455	291
28	1200	10	0.64	455	455	291
7	1400	0	0.56	547	547	306
7	1400	0	0.56	547	547	306
7	1400	0	0.56	547	547	306
28	1400	0	0.56	547	547	306
28	1400	0	0.56	547	547	306
28	1400	0	0.56	547	547	306
7	1400	0	0.6	538	538	323
7	1400	0	0.6	538	538	323
7	1400	0	0.6	538	538	323
28	1400	0	0.6	538	538	323
28	1400	0	0.6	538	538	323
28	1400	0	0.6	538	538	323
7	1400	0	0.64	530	530	339

7	1400	0	0.64	530	530	339
7	1400	0	0.64	530	530	339
28	1400	0	0.64	530	530	339
28	1400	0	0.64	530	530	339
28	1400	0	0.64	530	530	339
7	1400	2.5	0.56	547	547	306
7	1400	2.5	0.56	547	547	306
7	1400	2.5	0.56	547	547	306
28	1400	2.5	0.56	547	547	306
28	1400	2.5	0.56	547	547	306
28	1400	2.5	0.56	547	547	306
7	1400	2.5	0.6	538	538	323
7	1400	2.5	0.6	538	538	323
7	1400	2.5	0.6	538	538	323
28	1400	2.5	0.6	538	538	323
28	1400	2.5	0.6	538	538	323
28	1400	2.5	0.6	538	538	323
7	1400	2.5	0.64	530	530	339
7	1400	2.5	0.64	530	530	339
7	1400	2.5	0.64	530	530	339
28	1400	2.5	0.64	530	530	339
28	1400	2.5	0.64	530	530	339
28	1400	2.5	0.64	530	530	339
7	1400	5	0.56	547	547	306
7	1400	5	0.56	547	547	306
7	1400	5	0.56	547	547	306
28	1400	5	0.56	547	547	306
28	1400	5	0.56	547	547	306
28	1400	5	0.56	547	547	306
7	1400	5	0.6	538	538	323
7	1400	5	0.6	538	538	323
7	1400	5	0.6	538	538	323
28	1400	5	0.6	538	538	323
28	1400	5	0.6	538	538	323
28	1400	5	0.6	538	538	323
7	1400	5	0.64	530	530	339
7	1400	5	0.64	530	530	339
7	1400	5	0.64	530	530	339
28	1400	5	0.64	530	530	339
28	1400	5	0.64	530	530	339
28	1400	5	0.64	530	530	339
7	1400	7.5	0.56	547	547	306
7	1400	7.5	0.56	547	547	306
7	1400	7.5	0.56	547	547	306
28	1400	7.5	0.56	547	547	306
28	1400	7.5	0.56	547	547	306
28	1400	7.5	0.56	547	547	306
7	1400	7.5	0.6	538	538	323
7	1400	7.5	0.6	538	538	323
7	1400	7.5	0.6	538	538	323
28	1400	7.5	0.6	538	538	323
28	1400	7.5	0.6	538	538	323
28	1400	7.5	0.6	538	538	323
7	1400	7.5	0.64	530	530	339
7	1400	7.5	0.64	530	530	339
7	1400	7.5	0.64	530	530	339
28	1400	7.5	0.64	530	530	339
28	1400	7.5	0.64	530	530	339
28	1400	7.5	0.64	530	530	339

7	1400	10	0.56	547	547	306
7	1400	10	0.56	547	547	306
7	1400	10	0.56	547	547	306
28	1400	10	0.56	547	547	306
28	1400	10	0.56	547	547	306
28	1400	10	0.56	547	547	306
7	1400	10	0.6	538	538	323
7	1400	10	0.6	538	538	323
7	1400	10	0.6	538	538	323
28	1400	10	0.6	538	538	323
28	1400	10	0.6	538	538	323
28	1400	10	0.6	538	538	323
7	1400	10	0.64	530	530	339
7	1400	10	0.64	530	530	339
7	1400	10	0.64	530	530	339
28	1400	10	0.64	530	530	339
28	1400	10	0.64	530	530	339
28	1400	10	0.64	530	530	339